Design, synthesis, and biological evaluation of curcumin analogues as multifunctional agents for the treatment of Alzheimer's disease

ARTICLE *in* BIOORGANIC & MEDICINAL CHEMISTRY · JULY 2011

Impact Factor: 2.79 · DOI: 10.1016/j.bmc.2011.07.033 · Source: PubMed

8 AUTHORS, INCLUDING:

Jia-Heng Tan
Sun Yat-Sen University
84 PUBLICATIONS **1,333** CITATIONS
SEE PROFILE

Tian-Miao Ou
Sun Yat-Sen University
73 PUBLICATIONS **1,266** CITATIONS
SEE PROFILE

Zhishu Huang
Sun Yat-Sen University
174 PUBLICATIONS **2,282** CITATIONS
SEE PROFILE

Bioorganic & Medicinal Chemistry 19 (2011) 5596–5604

Contents lists available at ScienceDirect

Bioorganic & Medicinal Chemistry

journal homepage: www.elsevier.com/locate/bmc

Design, synthesis, and biological evaluation of curcumin analogues as multifunctional agents for the treatment of Alzheimer's disease

Shang-Ying Chen, Yuan Chen, Yan-Ping Li, Shu-Han Chen, Jia-Heng Tan *, Tian-Miao Ou, Lian-Quan Gu, Zhi-Shu Huang *

School of Pharmaceutical Sciences, Sun Yat-Sen University, Guangzhou 510006, People's Republic of China

ARTICLE INFO

Article history:
Received 12 May 2011
Revised 16 July 2011
Accepted 19 July 2011
Available online 24 July 2011

Keywords:
Curcumin analogue
Anti-Alzheimer agent
Aβ aggregation
Oxidative stress
Metal chelating

ABSTRACT

A series of novel curcumin analogues were designed, synthesized, and evaluated as potential multifunctional agents for the treatment of AD. The in vitro studies showed that these compounds had better inhibitory properties against Aβ aggregation than curcumin. Superior anti-oxidant properties (better than the reference compound Trolox) of these compounds were observed by the oxygen radical absorbance capacity (ORAC) method and a cell-based assay using DCFH-DA as a probe. In addition they were able to chelate metals such as iron and copper and decrease metal-induced Aβ aggregation. The structure–activity relationships were discussed. The results suggested that our curcumin analogues could be selected as multifunctional agents for further investigation of AD treatment.

1. Introduction

Alzheimer's disease (AD), a progressive neurodegenerative brain disorder, is affecting more and more elderly all around the world.[1] Data have revealed that there are 17 million AD patients until 2009 and the number would reach 70 million by 2050 if no cure or preventive measure is found.[2] The etiology of AD is still enigmatic, and multiple factors have been suggested to contribute to the development of AD. Amyloid-β (Aβ) plaques, widely accepted as the key pathological feature of AD, are mainly constituted by aggregation of the Aβ peptide, a 39- to 43-residue-long protein, derived from the amyloid precursor protein (APP).[3] Of two most abundant forms of Aβ, $Aβ_{1-42}$ has a higher propensity to form fibrils than $Aβ_{1-40}$. Furthermore, $Aβ_{1-42}$ aggregates into oligomers and fibrils in the brain and causes strong neuronal toxicity.[4] Prevention of Aβ aggregation in the brain is currently being considered as potential therapies for AD. Several series of inhibitors such as curcumin, rifampicin, benzofuran, and bis-styrylbenze analogues or derivatives were developed, and these compounds were found to interfere with fibrillization of Aβ.[5–8] Several studies suggested that oxidative damage also plays an important role in this chronic neurodegenerative disease.[9,10] The direct evidences of the oxidative stress hypothesis are increased lipid peroxidation and the increased concentration of Fe, Cu, Al, and Hg in AD patients' brian.[11] Thus, therapeutic strategy that aimed at the removal of free radicals or prevention of their formation might be beneficial for AD.

Recently, abundant data has implicated the roles of biometals such as iron, copper, and Zinc in the Aβ aggregate deposition and neurotoxicity including the formation of reactive oxygen species (ROS).[12,13] Firstly, abnormal enrichment of Cu, Fe, and Zn in postmortem AD brain has been confirmed.[14] In vitro experiments revealed that these metals are able to bind to Aβ, thus promoting its aggregation.[15] On the other hand, redox-active metal ions like Cu and Fe contribute to the production of ROS and widespread oxidation damages observed in AD brains.[16,17] Therefore, modulation of such biometals in the brain provides a potential therapeutic strategy for the treatment of AD. Small molecule chelating agents have been proposed for this purpose. In particular, Cu chelating agents have been widely explored to remove Cu from Cu-Aβ species and subsequently decrease metal-induced Aβ deposits.[18,19] The potential regulation of metal-induced Aβ aggregation and neurotoxicity through using traditional metal chelating agents, such as desferrioxamine, clioquinol (CQ), and 8-hydroxyquinoline derivative (PBT2) has been studied in clinical trials.[20–22] However, poor target specificity and consequential clinical safety of current metal-complexing agents make them undesirable for wide application. To circumvent this drawback, the new strategy of developing bifunctional or multifunctional metal chelators has recently been proposed.[23–25] In addition to the metal chelating ability, these agents are also designed to improve their uptake across the blood–brain barrier, decrease Aβ levels, inhibit cholinesterase and increase anti-oxidant capabilities.[25]

* Corresponding authors. Tel./fax: +86 20 39943056 (J.-H.T.).
E-mail addresses: tanjiah@mail.sysu.edu.cn (J.-H. Tan), ceshzs@mail.sysu.edu.cn (Z.-S. Huang).

0968-0896/$ - see front matter © 2011 Elsevier Ltd. All rights reserved.
doi:10.1016/j.bmc.2011.07.033

Indeed, the multifaceted condition of AD has encouraged active research in the development of multifunctional drugs with two or more complementary biological activities. Although a few noteworthy advances in the area of multifunctional agents have been achieved, the design of multifunctional drugs is still a tough work.[26,27] Clearly, the yield can be greatly increased by properly selecting the lead compound. Inspired by this concept, curcumin which already showed broad spectrum of biological activities related to AD was selected as the lead compound.[28] Curcumin is a yellowish polyphenol compound isolated from turmeric which might be responsible for the low age-adjusted prevalence of AD in India.[28] Various experiments demonstrate that curcumin has anti-oxidant, anti-inflammatory, anti-β-amyloid, and metal-chelating properties.[28,29] All these properties are critical in the pathogenesis of AD. In this work, we rationally designed the synthesized a novel series of curcumin analogues as multifunctional agents for the treatment of AD. Their biological evaluation includes inhibition of Aβ aggregation, anti-oxidant capabilities in vitro and in vivo, metal-chelating properties, and disassembly against metal-induced Aβ deposits.

2. Results and discussion

2.1. Design consideration and synthesis of curcumin analogues

In designing such curcumin analogues as multifunctional drugs, we focused on improving their inhibition activities of Aβ aggregation while retained the functional groups for anti-oxidation and metal chelation. As shown in Figure 1, the structure of curcumin is similar to that of the Congo Red and IMSB. They all have two aromatic end groups and a linker region in the middle.[30] It was referred that the two aromatic groups and their polar substitution are essential to their activities in terms of the efficient binding at the Aβ peptide guided by π-stacking and hydrogen bond interactions.[31] Therefore, we introduced an *N*-methylpiperazine on the two aromatic ends (Scheme 1) expecting that the hydrogen bonding substitutions and the additional electrostatic interactions would significantly strengthen the binding affinity to the Aβ peptide.[27,32] On the other hand, since it has been pointed out that the linkers are responsible for their activities.[31,33] Thus, we varied the flexibility of the linker as a key parameter for investigation. At the same time, most of the designed compounds retained carbonyl group which bears potential metal-chelating properties, along with the styryl function for their anti-oxidant activities.

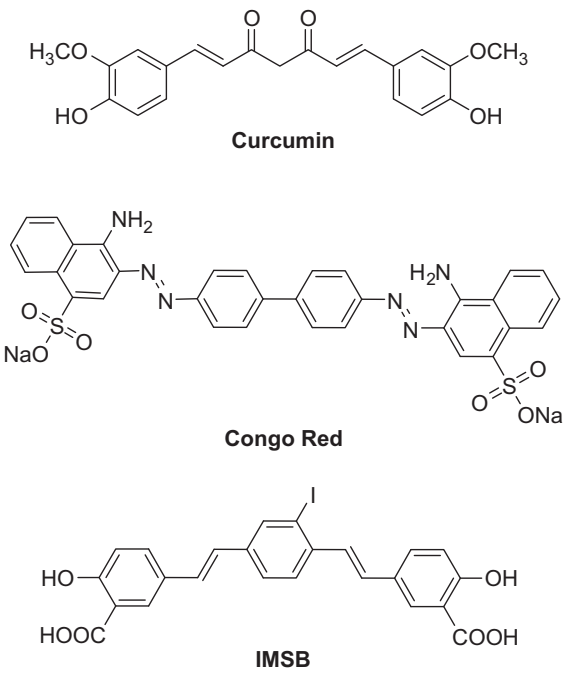

Figure 1. Structure of curcumin, Congo Red, and IMSB.

The facile synthetic pathway for curcumin analogues was illustrated in Scheme 1. Compounds **A1–A5**, **A9**–**A10**, and **B4** were synthesized by aldol reaction as reported.[34,35] Compound **A6** was obtained following the procedure of our previous work.[36] **A7** and **A8** were synthesized in accordance with the Kyung Hyun Lee method with little modification.[37] The configuration of the compounds was confirmed by the NOE analysis and coupling constant displaying that all compounds had linear (*E*, *E*) configuration.

2.2. Biological evaluation

2.2.1. Inhibition of self-mediated $A\beta_{1-42}$ aggregation

To investigate the self-mediated $A\beta_{1-42}$ aggregation, the Thioflavin T (ThT) fluorescence assay was performed. Inhibition activities of all substances against $A\beta_{1-42}$ aggregation were listed in Table 1 as IC_{50} and inhibition ratio at a tested concentration of 50 μM. Analysis of the data from ThT method revealed that all the tested compounds inhibited the Aβ aggregation while the inhibitory activities of these compounds vary accordingly. Compounds **A1–A6** with a chain of aliphatic structure displayed excellent IC_{50} values (ranging from 2–22 μM), while reduced inhibitory activity of **A7**–**A10**, with aromatous structure linkers in the middle was observed. These findings suggested that the flexibility of the chain between the two aromatic moieties might be an essential determinant of the compound's inhibitory activity as better inhibition properties can be obtained from the aliphatic structure linkers with less rigidity. Among **A1–A6**, compound **A4** was recognized by the most potent activity with an IC_{50} value of 2.5 μM and 90% inhibition at a concentration of 50 μM. Substitution with a carbon atom of the nitrogen atom or N-methylation in the linker of **A4** (see compound **A3** and **A5**) induced a lessening of activity, suggesting that piperidone structure fragment in the linker play a key role in the significant inhibition activity of the compound. Hereafter, compound **B4** with a similar structure of **A4** except a piperidine pattern in the two aromatic ends was designed to investigate the effect the terminal protonated nitrogen on $A\beta_{1-42}$ assembly. Although **B4** displayed less inhibitory potency against $A\beta_{1-42}$ aggregation, it still had a good inhibition of $A\beta_{1-42}$ aggregation with its IC_{50} value of 17.2 μM. Therefore, it indicated that the terminal protonated nitrogen in the ends may be less crucial than the linker for the inhibition activity of the compound.

2.2.2. Effect on Aβ β-sheet formation by A4

It was referred that $A\beta_{1-42}$ adopted a conformational mixture of α-helix, β-sheet, and random coil in the aqueous solution and underwent a conformational change to form intramolecular β-sheet structure in the fibrillation.[38] In order to further investigate the effect of the promising compound **A4** on the structural transition of $A\beta_{1-42}$, the CD spectroscopy method was employed to monitor the changes of the secondary structure of $A\beta_{1-42}$ during the assembly stages (0–32 h). Figure 2 showed that the contents of β-sheet structure (occurrence of a peak around 195 nm) and α-helix structure (occurrence of a broad minimum around 217 nm) increased during the first 32 h incubation (Fig. 2). Notably, the addition of compound **A4** resulted in a significant decrease in β-sheet structure at all tested time points during the first 32 h, but it had little effect on the content of α-helix structure, suggesting that **A4** may reduce or retard β-sheet structure formation through stabilizing the α-helix structure of peptide.

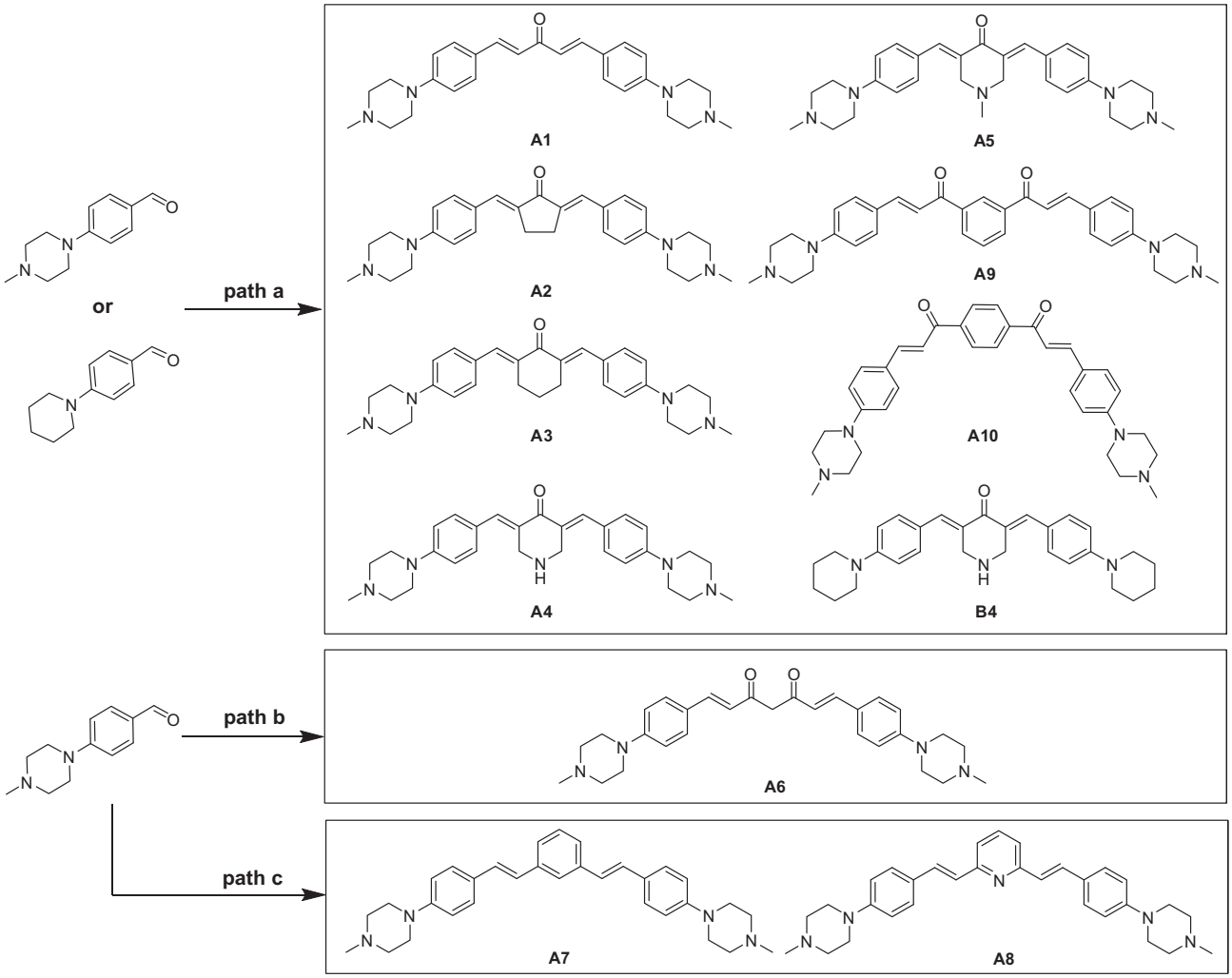

Scheme 1. Synthesis of curcumin analogues. Reagents and conditions: (a) ketone, 95% EtOH, 10% NaOH, rt, 30 min; or CH_3COOH, HCl, rt, 48 h; (b) acetylacetone, B_2O_3, *n*-$(BuO)_3B$, EtOAC, *n*-$C_4H_9NH_2$, 70 °C 24 h; (c) dibromide, potassium *t*-butoxide, THF, rt, 12 h.

Table 1
Inhibition of Aβ aggregation tested by ThT methods and ORAC values

Compounds	IC_{50}[a] (μM)	Inhibition of Aβ aggregation[b] (%)	ORAC[c]
A1	21.5 ± 3.7	68.6 ± 3.2	3.2 ± 0.2
A2	12.6 ± 3.9	67.2 ± 6.1	1.7 ± 0.2
A3	6.0 ± 4.1	73.1 ± 2.3	2.6 ± 0.2
A4	2.5 ± 1.2	90.2 ± 3.2	5.8 ± 0.1
A5	17.6 ± 2.7	65.1 ± 3. 5	4.7 ± 0.2
A6	9.2 ± 5.2	77.8 ± 2.2	1.9 ± 0.1
A7	>50	42.1 ± 2.0	1.2 ± 0.1
A8	>50	24.0 ± 5.2	1.1 ± 0.2
A9	37.8 ± 4.1	52.8 ± 2.7	1.3 ± 0.1
A10	>50	35.8 ± 1.9	1.1 ± 0.1
B4	17.2 ± 3.2	64.5 ± 3.3	2.4 ± 0.1
Curcumin	12.1 ± 1.2	71.3 ± 1. 3	2.5 ± 0.2
Trolox			1.00

[a] The Thioflavin-T fluorescence method was used. Values are expressed as the mean ± SD from at least two independent measurements.
[b] The maximum percent inhibition of aggregation in the ThT does dependence studies, all of them were found at the inhibitors' concentration of 50 μM.
[c] The mean ± SD of the three independent experiments and the measurements were carried out in presence of 0.625, 1.25, 2.5 μM compounds.

2.2.3. Effects on abundance of Aβ fibrils by A4

To complement the ThT binding assay and CD assay, $A\beta_{1-42}$ aggregation was also monitored by electron microscopy (EM). Substantial changes in the morphology of the aggregates were observed when $A\beta_{1-42}$ was incubated with **A4** (Fig. 3). At point 0, there was no aggregation for $A\beta_{1-42}$ with or without **A4**. However, after 12 h incubation, the sample of $A\beta_{1-42}$ alone had mostly aggregated into amyloid fibrils while less thin and short fibrils were caught in the sample of $A\beta_{1-42}$ in presence of **A4**. After 32 h incubation, numerous mature and bulky fibrils were observed in the sample of $A\beta_{1-42}$ alone. Meanwhile, only a few short fibrils and many breakage points were found in the $A\beta_{1-42}$ samples incubated with **A4**. The EM results were well consistent with the results of ThT and CD measurements, strongly proving that **A4** can inhibit and slow down the $A\beta_{1-42}$ fibrils formation.

2.2.4. Anti-oxidant activity in vitro

The reduction of the oxidative stress is another crucial aspect of designing the curcumin analogues. The oxygen radical absorbance capacity (ORAC) method was implemented to determine the anti-oxidant capacities of the synthesized compounds (Table 1). The ability to scavenge radicals is expressed as Trolox equivalent (their relative ability compared to the highly potent compound Trolox). From Table 1, it is quite evident that all the tested analogues had better anti-oxidant activities than Trolox. It's surprising to see several compounds (**A1**, **A3**–**A5**) even better than curcumin, since they lack the phenolic groups such as methoxy or hydroxyl, which are important for the anti-oxidant activities of curcumin. An

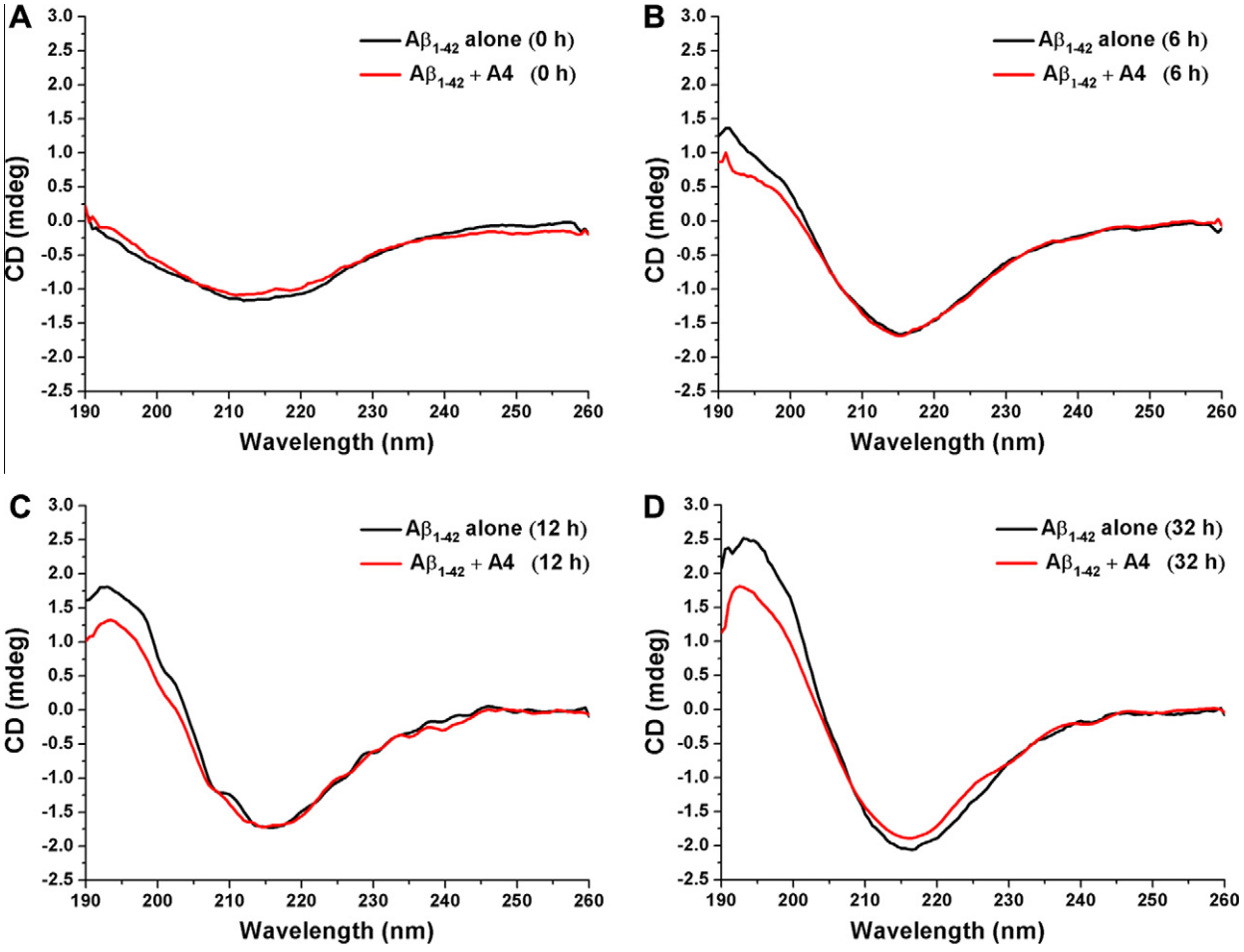

Figure 2. CD spectroscopy of $A\beta_{1-42}$ alone or with compound **A4** incubated at 0 h (A), 6 h (B), 12 h (C) and 32 h (D).

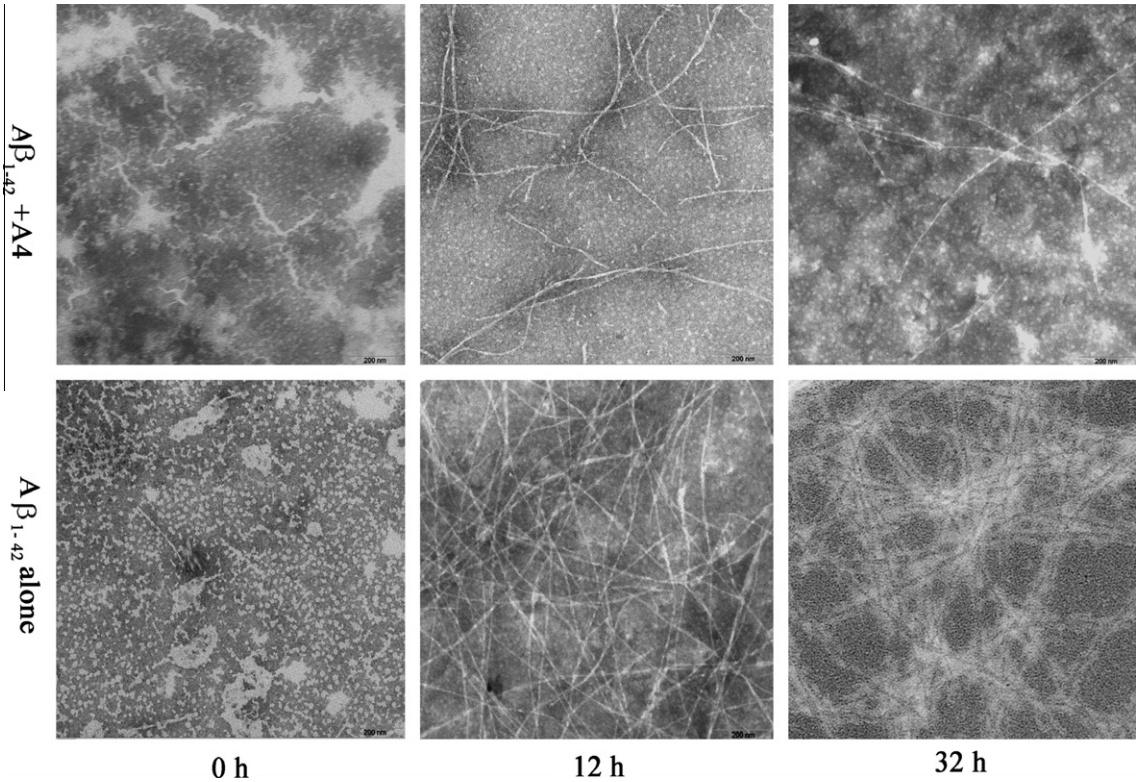

Figure 3. EM images of $A\beta_{1-42}$ (40 μM) in the presence and absence of 20 μM compound **A4**, after 0, 12, and 32 h of aggregation.

explanation for this might be that the styryl function and steric or electronic factors through the introduction of the piperazine groups contribute to their anti-oxidant activities. Furthermore, the trend of these compounds' anti-oxidant activities is similar to their inhibition activities of Aβ aggregation: compounds **A1–A6** exhibited better anti-oxidant activities than compounds **A7–A10** and among all the tested compounds, **A4** had the highest ORAC value (5.8), a much higher radical capture activity than Trolox (1.0) and curcumin (2.5). Therefore, it is clear that **A4** was more active than curcumin and other synthesized compounds in inhibiting Aβ fibril formation and scavenging radical.

2.2.5. Anti-oxidant activity in SH-SY5Y cells

The ability of the compounds to counteract the formation of ROS was assayed in human neuroblastoma cells (SH-SY5Y) after the treatment with *tert*-butyl hydroperoxide (*t*-BuOOH), a compound used to induce oxidative stress.[39] The concentration of tested compounds did not affect the cell viability (2.5 μM) (Fig. S1). As shown in Figure 4, the ROS levels of SH-SY5Y cells incubated with tested compounds decreased compared to control cells, particularly compounds **A1**–**A4**. Other anti-oxidants Trolox, N-acetyl-L-cysteine (NAC) and curcumin were also tested at a higher concentration (20 μM). As can be seen in Figure 4, NAC was unable to abolish ROS generation in SH-SY5Y cells treatment with *t*-BuOOH, while both Trolox and curcumin decreased the intensity of fluorescence. This result suggests that the action of these compounds involved in lipid peroxidation and free radical chain reaction might be close to that of Trolox.

2.2.6. Metal-chelating properties of A4

The chelation ability of compound **A4** toward biometals such as Cu, Fe and Zn was studied by UV–vis spectrometry.[40] Electronic spectral of compound **A4** in ethanol changed in the presence of Cu^{2+} and Fe^{2+} ions while remained unchanged after adding Zn^{2+} ions (Fig. 5). Upon the addition of $CuSO_4$ and $FeSO_4$, the curve had a red shift (after adding Cu^{2+}, the peak at 267 nm shift to 274 nm whereas the peak at 427 nm shift to 434 nm) suggesting the formation of complex **A4**-metal (II). However, after adding $ZnSO_4$, no significant difference was observed in the UV spectrum which indicates that this compound may not complex with zinc. Therefore, compound **A4** had the same selectivity of metal chelation as reported to curcumin (affinity for Cu^{2+} and Fe^{2+} rather than Zn^{2+}).[29]

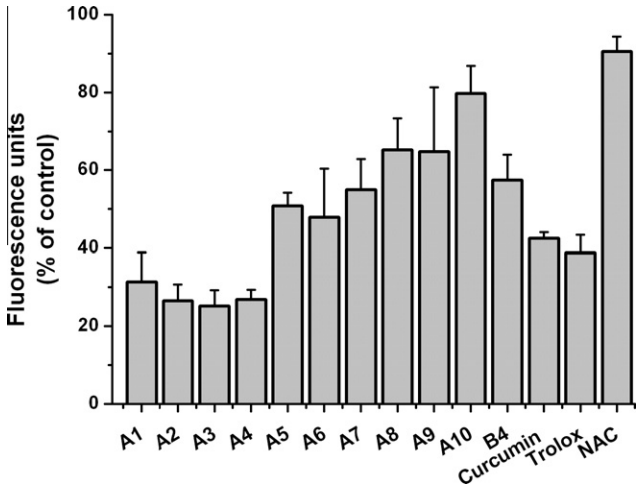

Figure 4. ROS generation in SH-SY5Y cells incubated without or with compounds measured using DCFH-DA. The results are expressed as the percentage of control cells (untreated with compounds).

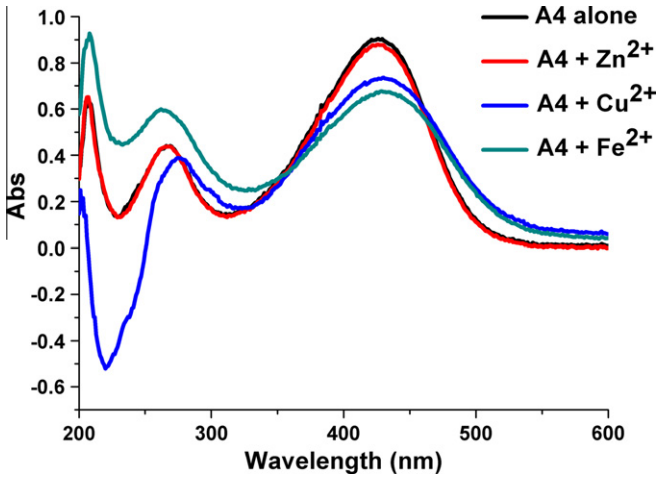

Figure 5. UV spectrum of compound **A4** (20 μM) alone or at the presence of 20 μM $ZnSO_4$, $CuSO_4$, and $FeSO_4$.

In order to determine the stoichiometry of the complex **A4**-metal (II), the molar ration method was employed, by preparing the solution of compound **A4** with ascending amounts of $CuSO_4$ or $FeSO_4$.[40] For instance, the UV spectra were recorded by numerical subtraction of $CuSO_4$ and **A4** at corresponding concentrations, and the spectra peaked at 493 nm (data not shown). According to Figure 6, it is implicit that the absorbance firstly increases at 493 nm and then tends to be stable versus the mole fraction of Cu^{2+} to **A4**. Therefore, two straight lines were draw with the intersection point at a mole fraction of 1.04, revealing 1:1 stoichiometry for metal(II)–ligand complexes. This is in accordance with other similar structures reported elsewhere.[29,40]

2.2.7. Effects on metal-induced $A\beta_{1-42}$ aggregation by A4

To investigate the impact of **A4** on metal-induced $A\beta_{1-42}$ aggregation, the ThT experiment was performed.[41] The general Aβ aggregation turbidity assay was not used because the absorbance of the **A4** and its corresponding metal complexes (see Fig. 5) overlapped the analysis window (405 nm) and significantly interfered with the result. ThT, however, showed a much higher fluorescent intensity than the compound and its metal complexes. For the disassembly of the metal fibril, all the samples containing Cu^{2+} and Fe^{2+} were buffered at pH 6.6, whereas the ones with Zn^{2+} were buffered at pH 7.4. The results were reported in Figure 7. Firstly, all three kinds of metal ions accelerated the aggregation of $A\beta_{1-42}$ in 45 min, while Fe^{2+} showed a

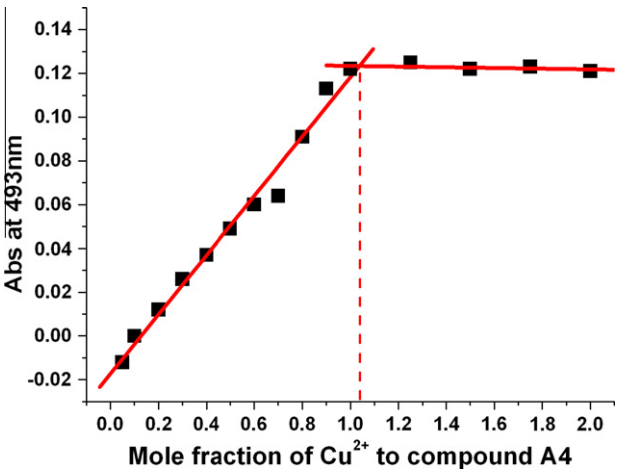

Figure 6. Determination of the stoichiometry of complex **A4**-Cu(II) by molar ration method.

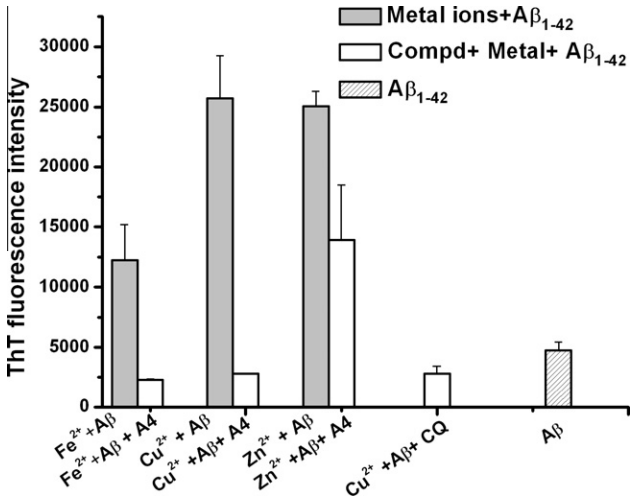

Figure 7. Influence of **A4** on metal-induced $A\beta_{1-42}$ aggregation. Values of ThT fluorescence intensity depicted in the figure were obtained by subtraction from that of the samples containing ThT solution and HEPEs buffer or the same concentrations of **A4**.

weaker ability of promoting $A\beta_{1-42}$ aggregation than Cu^{2+} and Zn^{2+}. Moreover, there was little aggregation of the $A\beta_{1-42}$ in the absence of metal ions after such short incubation time. Secondly, compound **A4** clearly decreased fibrils buildup in the presence of Cu^{2+} and Fe^{2+} compared with a potent Cu chelator CQ. And it had less inhibition effect on the Zn^{2+}-promoted fibrils, which was consistent with metal-chelating properties of **A4** (Fig. 5), selectively chelating to redox-active metal Fe and Cu, but not Zn. However, since **A4** also displayed inhibition of Zn^{2+}-promoted fibrils, suggesting that **A4** reduced metal-promoted fibril not only depending on its chelating ability.

3. Conclusions

In summary, a series of curcumin analogues have been designed, synthesized and evaluated as multifunctional anti-Alzheimer agents. Majority of the synthesized analogues displayed higher effective inhibitory potencies against Aβ aggregation than curcumin. Structure–activity relationships analysis for all synthesized analogues was investigated and the analysis suggested that the introduction of flexible moieties at the linker is crucial to the inhibitory potencies of the compounds against Aβ aggregation. Further investigations of compound **A4** by CD and EM experiments confirmed that **A4** can slow down or inhibit β-sheet aggregation and fibril formation. Furthermore, **A4** displayed better anti-oxidant property than the Trolox and curcumin. It also possessed the prospective property of acting as a metal chelator and inhibiting the metal-induced Aβ aggregation. These results strongly encourage further structure optimization of **A4** to develop more potent multifunctional anti-Alzheimer agents.

4. Experimental section

4.1. General

Commercially available reagents (chemicals) were used without further purification, unless otherwise stated. NMR spectra were recorded using TMS as the internal standard in $CDCl_3$ with a Bruker AvanceIII 400 spectrometer. Proton coupling patterns are described as single (s), double (d), triplet (t) and multiple (m). HRMS was obtained with an Agilent Iron-TOF-LC/MC spectrometer. The purities of synthesized compounds were confirmed by analytical HPLC performed with a LC-20A system equipped with a Ultimate-QB-C18 column (4.6 × 250 mm, 5 μm) and eluted with methanol/water (35:65–80:20) containing 0.1% TFA at a flow rate of 0.5 mL/min. Melting points (mp) were determined using a SRS-OptiMelt automated melting point instrument without correction.

4.2. Synthesis of curcumin analogues

4.2.1. (1*E*,4*E*)-1,5-Bis(4-(4-methylpiperazin-1-yl)phenyl)penta-1,4-dien-3-one (A1)

To a mixture of 4-(4-methylpiperazin-1-yl)benzaldehyde (204 mg, 1 mmol) and acetone (36 μL, 0.5 mmol) in 1 mL 95% ethanol, 0.5 mL 10% NaOH aqueous solution was added slowly at room temperature. The resulting reaction mixture was stirred for 30 min. The precipitate was then separated from solvent by filtration and washed with water to afford a yellow solid **A1** (179 mg, 85%); mp: 201–203 °C. ^{1}H NMR (400 MHz, $CDCl_3$) δ 7.60 (d, J = 15.8 Hz, 2H), 7.46 (d, J = 8.6 Hz, 4H), 6.84 (dd, J = 12.0 Hz, 8.8, 6H), 3.26 (t, J = 8.0 Hz, 8H), 2.52 (t, J = 8.0 Hz, 8H), 2.30 (s, 6H). ^{13}C NMR (100 MHz, $CDCl_3$) δ 187.80, 151.44, 141.65, 128.90, 124.43, 121.46, 113.85, 53.78, 46.73, 45.10. ESI-HRMS m/z: calcd for $C_{27}H_{34}N_4O$ $[M+H]^+$ 431.2811, found 431.2805.

4.2.2. (2*E*,5*E*)-2,5-Bis(4-(4-methylpiperazin-1-yl)benzylidene)-cyclopentanone (A2)

Following the method described for production of **A1**, a yellow solid **A2** (152 mg, 68%) was obtained; mp: 189–191 °C. ^{1}H NMR (400 MHz, $CDCl_3$) δ 7.46 (d, J = 9.0 Hz, 6H), 6.87 (d, J = 8.8 Hz, 4H), 3.26 (t, J = 8.0 Hz, 8H), 3.00 (s, 4H), 2.50 (t, J = 8.0 Hz, 8H), 2.29 (s, 6H). ^{13}C NMR (100 MHz, $CDCl_3$) δ 195.13, 150.35, 133.53, 132.27, 131.34, 125.71, 113.80, 53.81, 46.74, 45.12, 25.55. ESI-HRMS m/z: calcd for $C_{29}H_{36}N_4O$ $[M+H]^+$ 457.2967, found 457.2961.

4.2.3. (2*E*,6*E*)-2,6-Bis(4-(4-methylpiperazin-1-yl)benzylidene)-cyclohexanone (A3)

Following the method described for production of **A1**, a yellow solid **A3** (146 mg, 61%) was obtained; mp: 170–172 °C. ^{1}H NMR (400 MHz, $CDCl_3$) δ 7.68–7.65 (m, 2H), 7.36 (d, J = 8.7 Hz, 4H), 6.84 (d, J = 8.8 Hz, 4H), 3.24 (t, J = 8.0 Hz, 8H), 2.85 (t, J = 5.3 Hz, 4H), 2.50 (t, J = 8.0 Hz, 8H), 2.29 (s, 6H). ^{13}C NMR (100 MHz, $CDCl_3$) δ 189.06, 149.95, 135.65, 132.52, 131.14, 125.86, 113.67, 53.87, 46.94, 45.11, 27.63, 22.09. ESI-HRMS m/z: calcd for $C_{30}H_{38}N_4O$ $[M+H]^+$ 471.3124, found 471.3119.

4.2.4. (3*E*,5*E*)-3,5-Bis(4-(4-methylpiperazin-1-yl)benzylidene)-piperidin-4-one (A4)

Analog **A4** was obtained using an acid promoted aldol reaction (glacial acetic acid), following the procedure described by Adams.[35] Glacial acetic acid (8 mL) was saturated with HCl gas at room temperature, and then 4-piperidone hydrochloride monohydrate (192 mg, 1.25 mmol) was suspended. To the resulting clear solution, 4-(4-methylpiperazin-1-yl)benzaldehyde (510 mg, 2.5 mmol) was added and the reaction mixture was stirred for 3 days at room temperature. Then 10% NaOH was added to adjust the pH to 7, the forming yellow solids were filtered off, washed with water, and dried under vacuum yielding **A4** as yellow plates (315 mg, 67%); mp: 190–193 °C. ^{1}H NMR (400 MHz, $CDCl_3$) δ 7.67 (s, 2H), 7.27 (d, J = 8.8 Hz, 4H), 6.84 (d, J = 8.9 Hz, 4H), 4.09 (s, 4H), 3.25 (t, J = 8.0 Hz, 8H), 2.50 (t, J = 8.0 Hz, 8H), 2.29 (s, 6H). ^{13}C NMR (100 MHz, $CDCl_3$) δ 186.66, 150.25, 134.73, 131.36, 131.27, 124.93, 113.64, 53.83, 47.27, 46.77, 45.12. ESI-HRMS m/z: calcd for $C_{29}H_{37}N_5O$ $[M+H]^+$ 472.3076, found 472.3072.

4.2.5. (3*E*,5*E*)-1-Methyl-3,5-bis(4-(4-methylpiperazin-1-yl)benzylidene)piperidin-4-one (A5)

Following the method described for production of **A1**, a yellow solid **A5** (89 mg, 37%) was obtained; mp: 193–196 °C. ^{1}H NMR (400 MHz, $CDCl_3$) δ 7.67 (s, 2H), 7.26 (d, J = 8.8 Hz, 4H), 6.84

(d, J = 8.9 Hz, 4H), 3.70 (s, 4H), 3.29 (t, J = 8.0 Hz, 8H), 2.51 (t, J = 8.0 Hz, 8H), 2.39 (s, 3H), 2.27 (s, 6H). ^{13}C NMR (100 MHz, $CDCl_3$) δ 185.69, 150.19, 135.19, 131.26, 129.39, 125.01, 113.68, 56.26, 53.82, 46.76, 45.09, 44.81. ESI-HRMS m/z: calcd for $C_{30}H_{39}N_5O$ $[M+H]^+$ 486.3233, found 486.3225.

4.2.6. (1*E*,6*E*)-1,7-Bis(4-(4-methylpiperazin-1-yl)phenyl)hepta-1,6-diene-3,5-dione (A6)

Compound **A6** was prepared according to our previous Letter.[36] Boric anhydride (87 mg, 1.25 mmol) was suspended in 10 mL EtOAc in the presence of acetylacetone (251 mg, 2.5 mmol), and the mixture was stirred for 3 h at 70 °C. After evaporation of the solvent, the residue was washed with hexane and then, 5 mL EtOAc, 4-(4-methylpiperazin-1-yl) benzaldehyde (1.02 g, 5 mmol), and tributylborate (1.15 g, 5 mmol) were added, and the mixture was stirred for further 30 min. Butylamine (18 mg, 0.25 mmol) dissolved in EtOAc was added drop wise. The mixture acted at 70 °C for 24 h. Then 1 N HCl was added to adjust the pH to 5, and the solution was heated for 30 min at 60 °C. EtOAc was used to extract the product from the water layer. The compound **A6** was purified by recrystalization from EtOAc to yield yellow crystals (595 mg, 50%); mp: 214–216 °C. ^{1}H NMR (400 MHz, $CDCl_3$) δ 7.52 (d, J = 15.8 Hz, 2H), 7.41 (d, J = 13.2 Hz, 4H), 6.83 (d, J = 8.0 Hz, 4H), 6.39 (d, J = 15.7 Hz, 2H), 5.69 (s, 1H), 3.26 (t, J = 8.0 Hz, 8H), 2.51 (t, J = 8.0 Hz, 8H), 2.30 (s, 6H). ^{13}C NMR (100 MHz, $CDCl_3$) δ 182.30, 151.24, 139.22, 128.60, 124.69, 119.60, 113.94, 100.11, 53.83, 46.82, 45.12. ESI-HRMS m/z: calcd for $C_{29}H_{34}N_4O_2$ $[M+H]^+$ 473.2917, found 473.2911.

4.2.7. 1,3-Bis(4-(4-methylpiperazin-1-yl)styryl)benzene (A7)

The mixture of *m*-xylylene dibromide (625 mg, 2.5 mmol) and triethyl phosphate (1 mL, 5 mmol) was refluxed at 120 °C for 2 h. The reaction mixture was cooled to room temperature and then eluted with THF (50 mL), adding 570 mg (5 mmol) potassium *tert*-butoxide at 0 °C. After stirring for 20 min, 4-(4-methylpiperazin-1-yl)benzaldehyde (1.02 g, 5 mmol) was added and the reaction mixture was stirred for 30 min at room temperature. After slow addition of chilled water and stirred at room temperature for 30 min, the mixture was extracted with 30 mL ethylacetate twice. The combined organic layer was washed with saturated $NaHCO_3$ solution and brine, dried over $MgSO_4$, and concentrated to dryness to give a light yellow solid (199 mg, 17%); mp: 218–220 °C. ^{1}H NMR (400 MHz, $CDCl_3$) δ 7.51 (s, 1H), 7.37 (d, J = 8.7 Hz, 4H), 7.30–7.20 (m, 3H), 7.01 (d, J = 16.3 Hz, 2H), 6.90 (d, J = 16.3 Hz, 2H), 6.85 (d, J = 8.8 Hz, 4H), 3.23 (t, J = 8.0 Hz, 8H), 2.59 (t, J = 8.0 Hz, 8H), 2.34 (s, 6H). ^{13}C NMR (100 MHz, $CDCl_3$) δ 149.61, 137.13, 127.84, 127.75, 127.54, 126.48, 124.80, 123.86, 123.09, 114.80, 53.94, 47.60, 45.03. ESI-HRMS m/z: calcd for $C_{32}H_{38}N_4$ $[M+H]^+$ 479.3175, found 479.3183.

4.2.8. 2,6-Bis(4-(4-methylpiperazin-1-yl)styryl)pyridine (A8)

Following the method described for production of **A7**, a light yellow solid **A8** (102 mg, 8%) was obtained; mp: 212–214 °C. ^{1}H NMR (400 MHz, $CDCl_3$) δ 7.64–7.55 (m, 3H), 7.52 (d, J = 8.7 Hz, 4H), 7.20 (d, J = 16.1 Hz, 2H), 7.06 (d, J = 16.1 Hz, 2H), 6.92 (d, J = 8.8 Hz, 4H), 3.29 (t, J = 8.0 Hz, 8H), 2.60 (t, J = 8.0 Hz, 8H), 2.37 (s, 6H). ^{13}C NMR (100 MHz, $CDCl_3$) δ 155.90, 151.02, 136.64, 132.45, 128.19, 128.06, 125.51, 119.30, 115.52, 54.98, 50.76, 48.44, 46.09. ESI-HRMS m/z: calcd for $C_{31}H_{37}N_5$ $[M+H]^+$ 480.3127, found 480.3121.

4.2.9. (2*E*,2′*E*)-1,1′-(1,3-Phenylene)bis(3-(4-(4-methylpiperazin-1-yl)phenyl)prop-2-en-1-one) (A9)

Following the method described for production of **A1**, a yellow solid **A9** (154 mg, 57%) was obtained; mp: 216–218 °C. ^{1}H NMR (400 MHz, $CDCl_3$) δ 8.62–8.46 (m, 1H), 8.10 (dd, J = 15.6 Hz, 7.7 Hz, 2H), 7.73 (d, J = 12.8 Hz, 2H), 7.61–7.44 (m, 5H), 7.35 (d, J = 15.5 Hz, 2H), 6.85 (d, J = 11.4 Hz, 4H), 3.28 (t, J = 8.0 Hz, 8H), 2.51 (t, 8H), 2.29 (s, 6H). ^{13}C NMR (100 MHz, $CDCl_3$) δ 188.91, 151.78, 144.88, 138.12, 130.94, 129.39, 127.82, 127.02, 124.05, 116.89, 113.73, 53.74, 46.57, 45.07. ESI-HRMS m/z: calcd for $C_{34}H_{38}N_4O_2$ $[M+H]^+$ 535.3073, found 535.3068.

4.2.10. (2*E*,2′*E*)-1,1′-(1,4-Phenylene)bis(3-(4-(4-methylpiperazin-1-yl)phenyl)prop-2-en-1-one) (A10)

Following the method described for production of **A1**, a red solid **A10** (184 mg, 69%) was obtained; mp: 224–226 °C. ^{1}H NMR (400 MHz, $CDCl_3$) δ 8.01 (s, 4H), 7.72 (d, J = 15.6 Hz, 2H), 7.50 (d, J = 8.8 Hz, 4H), 7.30 (d, J = 15.6 Hz, 2H), 6.84 (d, J = 8.9 Hz, 4H), 3.30 (t, J = 8.0 Hz, 8H), 2.53 (t, J = 8.0 Hz, 8H), 2.31 (s, 6H). ^{13}C NMR (100 MHz, $CDCl_3$) δ 189.23, 151.80, 145.00, 140.66, 129.36, 127.45, 124.08, 113.79, 53.72, 46.55, 45.02. ESI-HRMS m/z: calcd for $C_{34}H_{38}N_4O_2$ $[M+H]^+$ 535.3073, found 535.3071.

4.2.11. (3*E*,5*E*)-3,5-Bis(4-(4-piperidin-1-yl)benzylidene)piperidin-4-one (B4)

Following the method described for production of **A4**, a red solid **B4** (174 mg, 32%) was obtained; mp: 208–210 °C. ^{1}H NMR (400 MHz, $CDCl_3$) δ 7.67 (s, 2H), 7.25 (d, J = 8.8 Hz, 4H), 6.83 (d, J = 8.8 Hz, 4H), 4.10 (s, 4H), 3.26–3.17 (t, J = 8.0 Hz, 8H), 1.69–1.50 (m, 12H). ^{13}C NMR (100 MHz, $CDCl_3$) δ 186.47, 150.81, 135.03, 131.48, 130.55, 124.05, 113.65, 48.10, 47.22, 24.47, 23.32. ESI-HRMS m/z: calcd for $C_{29}H_{35}N_3O$ $[M+H]^+$ 442.2858, found 442.2864.

4.3. Biological assay

4.3.1. ThT assay

Experiments were performed by incubating the peptides in 10 mM phosphate buffer (pH 7.4) at 37 °C for 48 h (final $A\beta_{1-42}$ 20 μM) with and without the tested compounds at different concentrations (2, 5, 10, 20, 50 μM). After incubation, the samples were diluted to a final volume of 180 μL with 50 mM glycine-NaOH buffer (pH 8.5) containing 5 μM Thioflavin T. Fluorescence signal was measured (excitation wavelength 450 nm, emission wavelength 485 nm and slit widths set to 5 nm) on a monochromators based multimode microplate reader (INFINITE M1000), adapted for 96-well microtiter plates. The fluorescence intensities were recorded, and the percentage of inhibition on aggregation was calculated by the following expression: $(1-I_{Fi}/I_{Fc}) \times 100\%$ in which I_{Fi} and I_{Fc} were the fluorescence intensities obtained for absorbance in the presence and absence of inhibitors, respectively, after subtracting the background fluorescence of the 5 μM Thioflavin T solution.

4.3.2. CD assay

$A\beta_{1-42}$ (20 μM) was mixed with and without 10 μM **A4** in 10 mM sodium phosphate buffer (pH 7.4). All solutions were incubated at 37 °C. CD spectra were obtained using a Jasco-810-150S spectropolarimeter (Jasco, Japan). A quartz cell with 1 mm optical path was used. Spectra were recorded at 25 °C between 190 and 260 nm with a bandwidth of 0.5 nm, a 3 s response time, and scan speed of 10 nm/min. Background spectra and when applicable, spectra of **A4** were subtracted.

4.3.3. EM study

$A\beta_{1-42}$ peptide (Anaspec Inc.) was dissolved in 10 mM phosphate buffer (pH 7.4) at 4 °C to give an 80 μM solution. $A\beta_{1-42}$ was incubated in the presence and absence of **A4** in 37 °C. The final concentrations of and **A4** were 40 μM and 20 μM, respectively. At specified time points, aliquots of 10 μL samples were placed on carbon-coated copper/rhodium grid. After 1 min, the

grid was washed with water and negatively stained with 2% uranyl acetate solution for 1 min. After draining off the excess of staining solution by means of a filter paper, the specimen was transferred for examination in a transmission electron microscope (JEOL JEM-1400).

4.3.4. Anti-oxidant activity in vitro-ORAC-FL assay

Compounds were directly dissolved in DMSO, and diluted with 75 mM potassium phosphate buffer (pH 7.4) for analysis. AAPH (0.414 g) was completely dissolved in 10 mL of 75 mM phosphate buffer (pH 7.4) to a final concentration of 40 mM. The unused AAPH solution was discarded within 8 h. Fluorescein stock solution (3.5 mM/L) was made in 75 mM phosphate buffer (pH 7.4) and was kept at 4 °C in dark condition. The fluorescein stock solution at such condition can last several months. The 140 nM fresh fluorescein working solution was made daily by further diluting the stock solution in 75 mM phosphate buffer (pH 7.4). Trolox standard was prepared as following: 0.25 g of Trolox was dissolved in 50 mL DMSO to give a 10 mM stock solution. The compounds and the Trolox stock solution were diluted with the same phosphate buffer to 25, 12.5, and 6.25 μM working solutions, and measured at final concentrations of, 2.5, 1.25, and 0.625 μM. All reaction mixtures were prepared fourfold and at least four independent runs were performed for each sample. Fluorescence measurements were normalized to the curve of the blank (without anti-oxidant). From the normalized curves, the area under the fluorescence decay curve (AUC) was calculated as:

(1) $$\mathrm{AUC} = 1 + \sum_{i=1}^{i=90} f_i/f_0$$

where f_0 is the initial fluorescence at 0 min and f_i is the fluorescence at time i. The net AUC for a sample was calculated as follows:

(2) Net AUC = $\mathrm{AUC_{anti\text{-}oxidant}} - \mathrm{AUC_{blank}}$. The ORAC-FL values were calculated.

(3) $[(\mathrm{auc_{sample}} - \mathrm{AUC_{blank}})/(\mathrm{AUC_{Trolox}} - \mathrm{AUC_{blank}})] \times$ [(concentration of Trolox/concentration of sample)] and expressed as Trolox equivalents by using the standard curve calculated for each assay. Final results were in μM of Trolox equivalent/μM of pure compound.

4.3.5. Anti-oxidant activity in SH-SY5Y Cells

Intracellular ROS were measured with the a fluorescent probe (2′,7′-dichlorofluorescein diacetate, DCFH-DA) as reported with some variation.[42,43] Human neuroblastoma cells, SH-SY5Y, were routinely grown at 37 °C in a humidified incubator with 5% CO_2 in Dulbecco's modified Eagle's medium (DMEM, GIBCO) containing 15 nonessential amino acid and supplemented with 10% fetal calf serum (FCS, GIBCO), 1 mM glutamine, 50 mg/μL penicillin, and 50 mg/μL streptomycin. For assays, SH-SY5Y Cells were sub-cultured in 96-well plates at a seeding density of 3×104 cells per well. After 24 h, they were treated with the synthesized compounds at concentrations of 2.5 μM. Concentrations of 2.5 μM compounds (final medium concentration: 0.05% DMSO) or vehicle as the control were used in an extensive study of the markers of cell death after 24 h exposure. After 24 h of treatment with the compounds, the cells were washed with PBS and then incubated with 5 μM DCFH-DA in PBS at 37 °C in 5% CO_2 for 30 min. After DCFH-DA was removed, the cells were washed and incubated with 0.1 mM *t*-BuOOH in PBS for 30 min. At the end of incubation, the fluorescence of the cells from each well was measured at 485 nm excitation and 535 nm emission with a monochromators based multimode microplate reader (INFINITE M1000).

4.3.6. Metal-chelating study

The chelating studies were made in ethanol using a UV–vis spectrophotometer (SHIMADZC UV-2450PC). The absorption spectral of compound **A4**, alone or in the presence of $CuSO_4$, $FeSO_4$, and $ZnCl_2$, was recorded at room temperature in a 1 cm quartz cell.

4.3.7. Effects of A4 on metal-induced $A\beta_{1-42}$ aggregation by ThT method

Two 4-(2-hydroxyethyl)-1-piperazineethanesulphonic acid (HEPES) buffer solutions (20 μM) containing 150 μM NaCl were prepared with distilled, deionized water at pH values of 6.6 and 7.4. Solutions of Fe^{2+} and Cu^{2+} were prepared from standards to final concentrations of 200 μM using the HEPES buffer at pH 6.6, and the Zn^{2+} solution was prepared to the same concentration with HEPES buffer at pH 7.4. Solutions of **A4** and CQ were prepared in DMSO in 10 mM for store, and diluted with HEPES buffer before use. To study effects of **A4** on the metal-induced $A\beta_{1-42}$ aggregation, $A\beta_{1-42}$ (20 μM) was co-incubated 40 μM Cu^{2+}, Fe^{2+}, and Zn^{2+} in HEPES buffer at pH 6.6 and 7.4, respectively, without or with compound **A4** (40 μM) or a potent metal chelator, CQ (40 μM). The incubation was performed at 37 °C for 45 min. After incubation, the samples were diluted to a final volume of 180 μL with 50 mM glycine–NaOH buffer (pH 8.5) containing 5 μM Thioflavin T. Fluorescence was measured at 450 nm (λ_{ex}) and 485 nm (λ_{em}) using a monochromators based multimode microplate reader (INFINITE M1000).

Acknowledgments

We thank the Natural Science Foundation of China (Grants U0832005, 90813011, 81001400), The International S&T Cooperation Program of China (2010DFA34630), The Specialized Research Fund for the Doctoral Program of Higher Education (20090171110050), and The Science Foundation of Guangzhou (2009A1-E011-6) for financial support of this study.

Supplementary data

Supplementary data associated with this article can be found, in the online version, at doi:10.1016/j.bmc.2011.07.033.

References and notes

1. Cummings, J. L. N. *Engl. J. Med.* **2004**, *351*, 56.
2. Alzheimer's Association. http://www.alz.org/national/documents/report_alzfactsfi-gures2009.pdf. **2009**.
3. Sommer, B. *Curr. Opin. Pharmacol.* **2002**, *2*, 87.
4. Selkoe, D. J. *Nature* **1999**, *399*, A23.
5. Ono, K.; Hasegawa, K.; Naiki, H.; Yamada, M. *Neurosci. Res.* **2004**, *75*, 742.
6. Narlawar, R.; Baumann, K.; Schubenel, R.; Schmidt, B. *Neurodegener. Dis.* **2007**, *4*, 88.
7. Byun, J. H.; Kim, H.; Kim, Y.; Mook-Jung, I.; Kim, D. J.; Lee, W. K.; Yoo, K. H. *Bioorg. Med. Chem. Lett.* **2008**, *18*, 5591.
8. Byeon, S. R.; Lee, J. H.; Sohn, J. H.; Kim, D. C.; Shin, K. J.; Yoo, K. H.; Mook-Jung, I.; Lee, W. K.; Kim, D. J. *Bioorg. Med. Chem. Lett.* **2007**, *17*, 1466.
9. Petersen, R. B.; Nunomura, A.; Lee, H. G.; Casadesus, G.; Perry, G.; Smith, M. A.; Zhu, X. *J. Alzheimers Dis.* **2007**, *11*, 143.
10. Praticò, D. *Trends Pharmacol. Sci.* **2008**, *29*, 609.
11. Markesbery, W. R. *Free Radical Biol. Med.* **1997**, *23*, 134.
12. Faller, P.; Hureau, C. *Dalton Trans.* **2009**, 1080.
13. Huang, X. D.; Atwood, C. S.; Hartshorn, M. A.; Multhaup, G.; Goldstein, L. E.; Scarpa, R. C.; Cuajungco, M. P.; Gray, D. N.; Lim, J.; Moir, R. D.; Tanzi, R. E.; Bush, A. I. *Biochemistry* **1999**, *38*, 7609.
14. Lovell, M. A.; Robertson, J. D.; Teesdale, W. J.; Campbell, J. L.; Markesbery, W. R. *J. Neurol. Sci.* **1998**, *158*, 47.
15. Smith, D. G.; Cappai, R.; Barnham, K. J. *Biochim. Biophys. Acta* **2007**, *1768*, 1976.
16. Pierre, J. L.; Fontecave, M. *Biometals* **1999**, *12*, 195.
17. Fernández-Bachiller, M. I.; Pérez, C.; Campillo, N. E.; Páez, J. A.; González-Muñoz, G. C.; Usán, P.; García-Palomero, E.; López, M. G.; Villarroya, M.; García, A. G.; Martínez, A.; Rodríguez-Franco, M. I. *ChemMedChem* **2009**, *4*, 828.
18. Hindo, S. S.; Mancino, A. M.; Braymer, J. J.; Liu, Y.; Vivekanandan, S.; Ramamoorthy, A.; Lim, M. H. *J. Am. Chem. Soc.* **2009**, *131*, 16663.

19. Wu, W. H.; Lei, P.; Liu, Q.; Hu, J.; Gunn, A. P.; Chen, M. S.; Rui, Y. F.; Su, X. Y.; Xie, Z. P.; Zhao, Y. F.; Bush, A. I.; Li, Y. M. *J. Biol. Chem.* **2008**, *283*, 31657.
20. Crapper McLachlan, D. R.; Dalton, A. J.; Kruck, T. P.; Bell, M. Y.; Smith, W. L.; Kalow, W.; Andrews, D. F. *Lancet* **1991**, *337*, 1304.
21. Ritchie, C. W.; Bush, A. I.; Mackinnon, A.; Macfarlane, S.; Mastwyk, M.; MacGregor, L.; Kiers, L.; Cherny, R.; Li, Q. X.; Tammer, A.; Carrington, D.; Mavros, C.; Volitakis, I.; Xilinas, M.; Ames, D.; Davis, S.; Beyreuther, K.; Tanzi, R. E.; Masters, C. L. *Arch. Neurol.* **2003**, *60*, 1685.
22. Lannfelt, L.; Blennow, K.; Zetterberg, H.; Batsman, S.; Ames, D.; Harrison, J.; Masters, C. L.; Targum, S.; Bush, A. I.; Murdoch, R.; Wilson, J.; Ritchie, C. W. *Lancet Neurol.* **2008**, *7*, 779.
23. Dedeoglu, A.; Cormier, K.; Payton, S.; Tseitlin, K. A.; Kremsky, J. N.; Lai, L.; Li, X. H.; Moir, R. D.; Tanzi, R. E.; Bush, A. I.; Kowall, N. W.; Rogers, J. T.; Huang, X. D. *Exp. Gerontol.* **2004**, *39*, 1641.
24. Choi, J. S.; Braymer, J. J.; Nanga, R. P. R.; Ramamoorthy, A.; Lim, M. H. *Proc. Natl. Acad. Sci. U.S.A.* **2010**, *107*, 21990.
25. Perez, L. R.; Franz, K. J. *Dalton Trans.* **2010**, *39*, 2177.
26. Fang, L.; Kraus, B.; Lehmann, J.; Heilmann, J.; Zhang, Y. H.; Decker, M. *Bioorg. Med. Chem. Lett.* **2008**, *18*, 2905.
27. Kapková, P.; Alptüzün, V.; Frey, P.; Erciyas, E.; Holzgrabe, U. *Bioorg. Med. Chem.* **2006**, *14*, 472.
28. Hamaguchi, T.; Ono, K.; Yamada, M. C. N. S. *Neurosci. Ther.* **2010**, *16*, 285.
29. Baum, L.; Ng, A. *J. Alzheimers Dis.* **2004**, *6*, 367.
30. Yang, F. S.; Lim, G. P.; Begum, A. N.; Ubeda, O. J.; Simmons, M. R.; Ambegaokar, S. S.; Chen, P. P.; Kayed, R.; Glabe, C. G.; Frautschy, S. A.; Cole, G. M. *J. Biol. Chem.* **2005**, *280*, 5892.
31. Reinke, A. A.; Gestwicki, J. E. *Chem. Biol. Drug Des.* **2007**, *70*, 206.
32. Salomon, A. R.; Marcinowski, K. J.; Friedland, R. P.; Zagorski, M. G. *Biochemistry* **1996**, *35*, 13568.
33. Simons, L. J.; Caprathe, B. W.; Callahan, M.; Graham, J. M.; Kimura, T.; Lai, Y. J.; LeVine, H.; Lipinski, W.; Sakkab, A. T.; Tasaki, Y.; Walker, L. C.; Yasunaga, T.; Ye, Y. Y.; Zhuang, N.; Augelli-Szafran, C. E. *Bioorg. Med. Chem. Lett.* **2009**, *19*, 654.
34. Peng, D.; Tan, J. H.; Chen, S. B.; Ou, T. M.; Gu, L. Q.; Huang, Z. S. *Bioorg. Med. Chem.* **2010**, *18*, 8235.
35. Adams, B. K.; Ferstl, E. M.; Davis, M. C.; Herold, M.; Kurtkaya, S.; Camalier, R. F.; Hollingshead, M. G.; Kaur, G.; Sausville, E. A.; Rickles, F. R.; Snyder, J. P.; Liotta, D. C.; Shoji, M. *Bioorg. Med. Chem.* **2004**, *12*, 3871.
36. Qiu, X.; Liu, Z.; Shao, W. Y.; Liu, X.; Jing, D. P.; Yu, Y. J.; An, L. K.; Huang, S. L.; Bu, X. Z.; Huang, Z. S.; Gu, L. Q. *Bioorg. Med. Chem.* **2008**, *16*, 8035.
37. Lee, K. H.; Shin, B. H.; Shin, K. J.; Kim, D. J.; Yu, J. *Biochem. Biophys. Res. Commun.* **2005**, *328*, 816.
38. Pratim Bose, P.; Chatterjee, U.; Nerelius, C.; Govender, T.; Norstrom, T.; Gogoll, A.; Sandegren, A.; Gothelid, E.; Johansson, J.; Arvidsson, P. I. *J. Med. Chem.* **2009**, *52*, 8002.
39. Oyama, Y.; Hayashi, A.; Ueha, T.; Maekawa, K. *Brain Res.* **1994**, *635*, 113.
40. Bolognesi, M. L.; Cavalli, A.; Valgimigli, L.; Bartolini, M.; Rosini, M.; Andrisano, V.; Recanatini, M.; Melchiorre, C. *J. Med. Chem.* **2007**, *50*, 6446.
41. Raman, B.; Ban, T.; Yamaguchi, K.; Sakai, M.; Kawai, T.; Naiki, H.; Goto, Y. *J. Biol. Chem.* **2005**, *280*, 16157.
42. Zhang, S. J.; Lenhart, J. A.; Ling, X. A.; Gandhi, R.; Guo, T. L.; Gerk, P. M.; Brunzell, D. H. *J. Med. Chem.* **2010**, *53*, 6198.
43. Bolognesi, M. L.; Banzi, R.; Bartolini, M.; Cavalli, A.; Tarozzi, A.; Andrisano, V.; Minarini, A.; Rosini, M.; Tumiatti, V.; Bergamini, C.; Fato, R.; Lenaz, G.; Hrelia, P.; Cattaneo, A.; Recanatini, M.; Melchiorre, C. *J. Med. Chem.* **2007**, *50*, 4882.